Colloids and Surfaces A: Physicochemical and Engineering Aspects 728 (2026) 138537

Contents lists available at ScienceDirect

Colloids and Surfaces A: Physicochemical and Engineering Aspects

journal homepage: www.elsevier.com/locate/colsurfa

A prediction model of the stability reduction performance of aqueous film forming foam based on high-low temperature alternating aging test

Biao Zhou [a,*], Junyi Zhang [a], Qihang Yue [a], Kai Wang [a], Hideki Yoshioka [b], Peiyao Chen [c], Zhengyang Wang [d], Wei Wang [d], Yafei Zhou [e], Shanlong Wang [f]

[a] School of Emergency Management and Safety Engineering, China University of Mining and Technology (Beijing), Beijing 100083, China
[b] Department of Architecture, Faculty of Engineering, The University of Tokyo, Tokyo 113-8654, Japan
[c] Tianjin Fire Science and Technology Research Institute of MEM, Tianjin 300381, China
[d] Shanghai Fire Science Technology Research Institute of MEM, Shanghai 200032, China
[e] China Waterborne Transport Research Institute, Beijing 100088, China
[f] Ministry of Emergency Management of the People's Republic of China, Beijing 100713, China

GRAPHICAL ABSTRACT

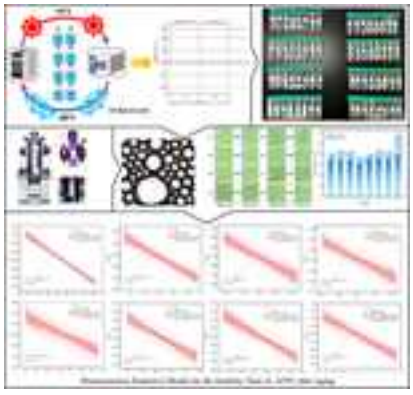

ARTICLE INFO

Keywords:
Firefighting foam
Accelerated aging
Foam analyzer
Temperature cycling
Prediction Model

ABSTRACT

In this paper, high and low temperature alternating accelerated aging tests were carried out on the aqueous film-forming foam fire extinguishing agent (AFFF) at a low temperature of −40 ℃ and a high temperature of 55 ℃. A ring tensiometer and a viscometer were used to measure the surface tension and viscosity of the foam. The Dynamic Foam Analyzer (DFA100) monitored foam evolution in real time using a high-speed camera to investigate the performance changes of AFFF after aging. The results show that under the alternating aging at low temperature −40 ℃ and high temperature 55 ℃. The drainage performance, foaming capacity, and microstructural stability of various foam types were all negatively affected. In particular, the standardized foam drainage rate increased by 0.22–1.73 times, the expansion ratio decreased by 4–14 %, and the foam stability time declined by 0.79–2.8 %. A dimensionless prediction model for the stability time of AFFF after aging was established based on the key performance parameters of foam.

* Corresponding author.
E-mail address: zhoubiao1088@cumtb.edu.cn (B. Zhou).

https://doi.org/10.1016/j.colsurfa.2025.138537
Received 29 July 2025; Received in revised form 16 September 2025; Accepted 1 October 2025
Available online 3 October 2025

1. Introduction

With the rise and development of the petrochemical industry, the use of liquid fuels has become increasingly widespread, and their varieties have grown significantly [1]. During the storage of liquid fuels, potential hazards such as oil leakage, fires, and explosions may occur due to container corrosion, lightning, and other factors [2]. Aqueous Film-Forming Foam (AFFF) is an efficient extinguishing agent for organic fuel fires. It primarily composed of fluorocarbon surfactants and hydrocarbon surfactants. Generally, functional additives such as viscosity enhancers, pour point depressants, and preservatives are added [3,4]. By using surfactants, the surface tension of the liquid is reduced, forming a water film and foam layer that covers the entire surface of the liquid fuel. This isolates oxygen while absorbing heat generated during combustion, thereby achieving the extinguishing effect [5]. Since AFFF requires long-term storage, it inevitably faces the issue of aging and degradation during storage [6]. Therefore, it is of great significance to study the stability of AFFF during storage and the changes in its foam performance.

In recent years, many researchers have studied the performance of AFFF. The research primarily focuses on the effects of mixed types and proportions of foaming agents on foam performance [7], the influence of different surfactants [8–10] and foam stabilizers on foam performance [11,12], and the impact of storage equipment on AFFF performance parameters in aviation firefighting [13]. In addition, the comparison of drainage performance characteristics of different types of foams [14,15], the dynamic surface and interfacial tension of different foam solutions [16], and the effects of salts on the fire extinguishing performance of AFFF have also been studied [17,18]. The research on the effect of aging on the performance of AFFF is mainly aimed at the effect of a single thermal aging mechanism on the performance of AFFF. The current research mainly includes: the analysis of parameters such as viscosity, static and dynamic surface tension, capillary shape and pressure distribution during foam aging, and the summary of the distribution law of boundary pressure in the stable stage before and after aging [19]. AFFF was thermally aged using a cone calorimeter, and the effects of thermal radiation on drainage time, foam evaporation and foam attenuation characteristics before and after aging of AFFF were compared [6]. By heating the extinguishing agent to simulate its effective service life, the effects of thermal aging on the foam expansion ratio, drainage time, and extinguishing efficiency of fluor protein foam (FP), AFFF, and alcohol-resistant aqueous film-forming foam (AFFF/AR) were analyzed [20]. So far, research has primarily focused on the effects of a single thermal aging mechanism on various performance parameters of AFFF.

Fig. 1. Different types of foam samples.

However, there is almost no research on high-low temperature alternating aging of AFFF.

Therefore, this study experimentally investigates the evolution patterns of foam drainage performance, foaming ability, and microstructural stability under high-low temperature alternating aging cycles. A dimensionless predictive model for the stability time of aged AFFF is established. Through this study, it is hoped that a certain theoretical reference can be provided for the evolution of foam performance during AFFF storage.

2. Experiment and method

2.1. Materials

Due to its low surface tension, AFFF exhibits rapid fire extinguishing speed, strong sealing properties, and excellent resistance to reignition. It forms a water film on the fuel surface and, through the combined action of foam and the water film, is widely used in flammable liquid fires and large storage tank fires. This study aims to investigate the overall performance variation trends of commonly used AFFF products before and after high–low temperature alternating aging. Since the primary components of the selected samples are largely consistent, the minor variations in component proportions are not considered within the scope of this study. The experiment selected eight different types of AFFF. S1 is 6 % AFFF, S2 is 3 % AFFF, S3 is 6 % AFFF, S4 is 3 % AFFF, S5 is 3 % Seawater AFFF, S6 is 6 % Seawater AFFF, S7 is 6 % Seawater resistant AFFF, S8 is 1 %AFFF. These samples represent commonly available AFFF and AFFF/AR products on the market and have significant application value. They enable a comprehensive evaluation of the effects of high-low temperature alternating aging on foam performance and enhance the practical significance of the research findings.

2.2. Experimental equipment

2.2.1. High-low temperature alternating aging test equipment

The foam aging test is conducted under alternating high and low temperature conditions, as shown in Fig. 2. The high-temperature heating test is conducted using an electric blast drying oven, which primarily consists of heating elements, a fan, and a control panel. By setting appropriate parameters, the foam solution inside the chamber is subjected to heating treatment. The low temperature freezing test is conducted using a low temperature freezer, which mainly comprises a refrigeration system and a control system. By setting the desired temperature, the foam solution inside the chamber is subjected to low-temperature treatment. During the alternating high and low temperature aging process, the sample will transition from liquid to solid and back to liquid. This is because at −40 ℃, the water and hydrophilic components in the sample solution crystallize, making the sample solid. At 50 ℃, these components dissolve, and the sample returns to liquid form.

2.2.2. Dynamic foam analyzer

Foam performance tests were conducted using the Dynamic Foam Analyzer (DFA100) manufactured by Kruss, as shown in Fig. 3. The analyzer primarily consists of a prism measurement column, electrode plates, a data acquisition system, and a high-definition video camera. The instrument uses light-emitting and photosensitive elements to capture the changes in the phase interface between air and foam, and between foam and liquid in real time, and obtain the foam structure stability and foaming performance. The gas-liquid ratio was controlled and maintained by the built-in flow regulation system of the foam analyzer. The liquid volume was precisely set using the instrument's metering pump, while the gas volume was adjusted and stabilized through a calibrated mass flow controller. The analyzer continuously monitors the input gas and liquid flow rates during operation, ensuring that the gas-liquid ratio remains constant at throughout the test. Before

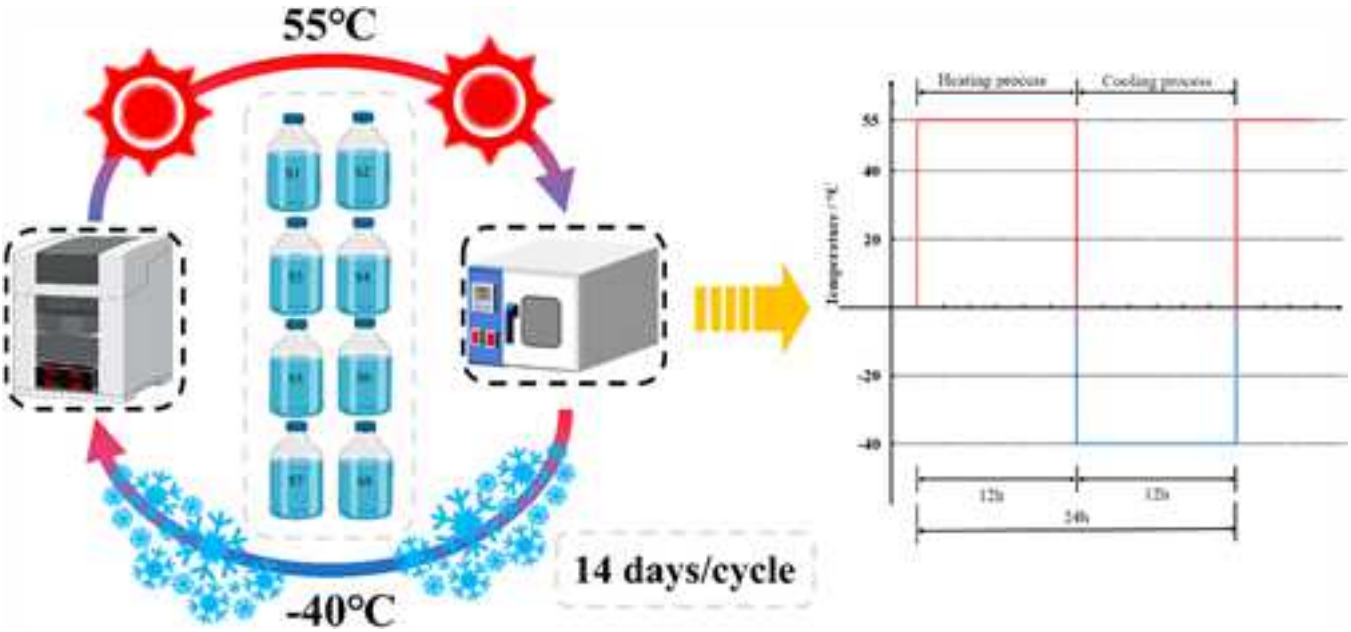

Fig. 2. High-low temperature alternating aging flow chart.

Fig. 3. The configuration of Dynamic Foam Analyzer.

starting the test, the height illumination and structural illumination values need to be adjusted to appropriate levels. The high-definition video camera indirectly reflects foam size by capturing changes in foam projections. By setting appropriate parameters, the foam solution within the prism measurement column was foamed and simultaneously analyzed for foam performance.

2.2.3. Ring tensiometer

The measurement methods for liquid surface tension include the capillary rise method, Wilhelmy plate method, drop shape analysis, and ring method. In this study, the surface tension of AFFF was measured using the KSV Sigma 700 tensiometer, as shown in Fig. 4. The operating principle of this tensiometer is based on the ring method, utilizing a platinum ring for measurement. During the experiment, the platinum ring is lowered uniformly into the liquid surface and then raised at a constant speed. As it rises, it experiences a downward force due to the surface tension of the solution. The measurement is recorded when the force reaches equilibrium, providing the surface tension value of the solution.

2.2.4. Viscometer

The tested foam extinguishing solutions are essentially non-Newtonian fluids. Since their viscosity continuously changes under different conditions, measurements were taken only after the readings stabilized, representing the dynamic viscosity of the non-Newtonian fluid. In this study, the viscosity of AFFF was measured using a Brookfield DV1 viscometer, as shown in Fig. 5.

Fig. 4. The figure of surface tensiometer and testing principle.

Fig. 5. The figure of Viscometer.

2.3. Foam high-low temperature alternating aging test

According to the AFFF high and low temperature alternating aging test protocol, 8 types of AFFF are packed in sealed glass sample bottles. The samples are placed in an electric blast drying oven and heated at (55 ± 0.2) ℃ for 12 h. After heating, they are transferred to a low temperature freezer and maintained at (-40 ± 0.2) ℃ for 12 h. A 14 d period is defined as one aging cycle, and the process is repeated accordingly. At the end of each cycle, 50 ml of each foam sample is collected for foam performance testing.

2.4. Foam performance test

The parameters of the dynamic foam analyzer are set as follows: a gas-to-liquid ratio of 6:1, a pumped gas volume of 120 ml, a gas flow rate of 0.3 L/min, a height illumination of 12 %, and a structural illumination of 23–25 %. After all devices are installed and calibrated, the experiment was initiated. A total of 20 ml of the prepared foam solution is injected into the prism measurement column. All parameters are adjusted, and the dynamic foam analyzer is activated. The foaming process is observed for any occurrences of gas leakage. Finally, the foam performance test results are recorded, and the data is saved.

Before the experiment, the weighing accuracy of the balance hook is calibrated using standard weights. The platinum ring is cleaned with deionized water and then heated with an alcohol lamp until it turned red to remove surface-active substances. After cooling, the platinum ring is securely attached to the balance hook. During the experiment, the platinum ring is lowered until it is immersed in the surface layer of the AFFF solution, then raised until it reaches a stationary position. At this point, the reading on the surface tensiometer represents the surface tension of the AFFF solution.

The viscometer speed is set to 60 RPM for the experiment. After wetting the rotor and rotor guard with the test solution, 20–30 ml of the solution is added. The measurement is initiated, and once the readings stabilize, the viscosity values of different types of AFFF are recorded.

3. Results and discussion

3.1. Effect of high-low temperature alternating aging on foam drainage performance

Foam drainage rate is an important indicator for measuring the water retention capacity and flow properties of foam [21]. To comprehensively evaluate the effect of aging on the drainage performance of foam, a more comprehensive characterization can be obtained by analyzing the three indicators of foam drainage rate (75 % standardized drainage rate), moisture content and initial Sauter radius.

The 75 % standardized drainage rate can be calculated by the following formula:

$$S = V_d / A \bullet t \tag{1}$$

Where: S is the 75 % standardized drainage rate, L/(m^2·s); V_d is the drainage volume, L; A is the foam surface area, m^2; t is 75 % drainage, s.

The moisture content can be calculated by the following formula:

$$MC = V_{foam} - V_d / V_{foam} \times 100\% \tag{2}$$

Where: MC is the moisture content, %; V_{foam} is the initial foam volume, L.

The initial Sauter radius can be calculated by the following formula:

$$r_{32initial} = \sum n_i r_i^3 \Big/ \sum n_i r_i^2 \tag{3}$$

Where: $r_{32\ initial}$ is initial Sauter mean radius, μm; n_i is the initial foam bubble number; r_i is the initial foam bubble radius, μm.

During the high-temperature heating process, the loss of solvent components was negligible due to the good sealing performance of the container. After freezing, the sample changed from solid to liquid, and there was no obvious change in color. During the experiment, floccules were observed in the solution, which may be formed by precipitation and aggregation of solution components. This indicates that the uniformity of the solution is destroyed [22–24]. However, the high-temperature aging conditions do not reach the degradation temperature of the surfactants. Therefore, theoretically, no toxic substances are produced during the aging process [25]. Details are shown in Fig. 6.

As shown in Fig. 7, with the increase of aging cycle, the drainage rate of the samples showed an upward trend. At the same time, the water

Fig. 6. The apparent changes and phase transitions of the sample.

content showed a downward trend with the increase of drainage rate. It is worth noting that the changes in S1, S2, and S6 are the most significant, with drainage rates increasing by 1.73 times, 0.62 times, and 0.99 times, respectively, and the foam drainage stability is poor. At the same time, the liquid content decreased by 92.4 %, 60.3 %, and 44.8 % respectively compared with the initial value.

As shown in Fig. 8, the overall initial Sauter mean radius exhibits an increasing trend with the progression of the aging cycle. Among them, sample S8 had the largest initial Sauter radius before the experiment. It increased significantly with the aging cycle, reaching a growth of approximately 50 % by the end of the test, indicating poor aging resistance. Sample S4 had the smallest initial Sauter radius, with a growth of only 23.3 % over the entire aging cycle, demonstrating superior aging resistance. The Sauter radius of the remaining samples varied between 14.5 % and 27.9 %, indicating a moderate level of aging resistance.

As analyzed in the previous article, there are component aggregation and uneven concentration distribution in the foam solution. In areas with excessively high concentrations, the viscosity of the solution increases, resulting in increased resistance to bubble formation and a decrease in the number of bubbles generated [26]. In areas with too low concentrations, the strength of the bubble liquid film generated is low and difficult to maintain. At the same time, the uniformity of the generated bubbles is greatly affected, which further accelerates the speed of gravity drainage and bubble rupture, resulting in an increase in drainage rate, a decrease in water content, and an increase in the initial Sauter radius. The decline in foam water retention is also related to changes in foam additives. High temperature accelerates the migration and rearrangement of surfactants in the foam solution, destroying the structural integrity of the liquid film. Low temperature cause components to freeze or precipitate, further weakening the stability of the film and the intermolecular forces between foam sheets. During the high and low temperature alternating aging process, the foam liquid film is repeatedly destroyed [22–24,26]. The liquid is easier to discharge from the foam, the drainage rate is accelerated, the liquid content is reduced, and the initial Sauter radius is increased. These phenomena indicate a significant decrease in the foam's drainage performance. As liquid loss accelerates between the bubbles, the foam's overall collapse rate increases, making it difficult to form a stable and durable coating on the fuel surface, thereby weakening the foam's cooling effect on the liquid

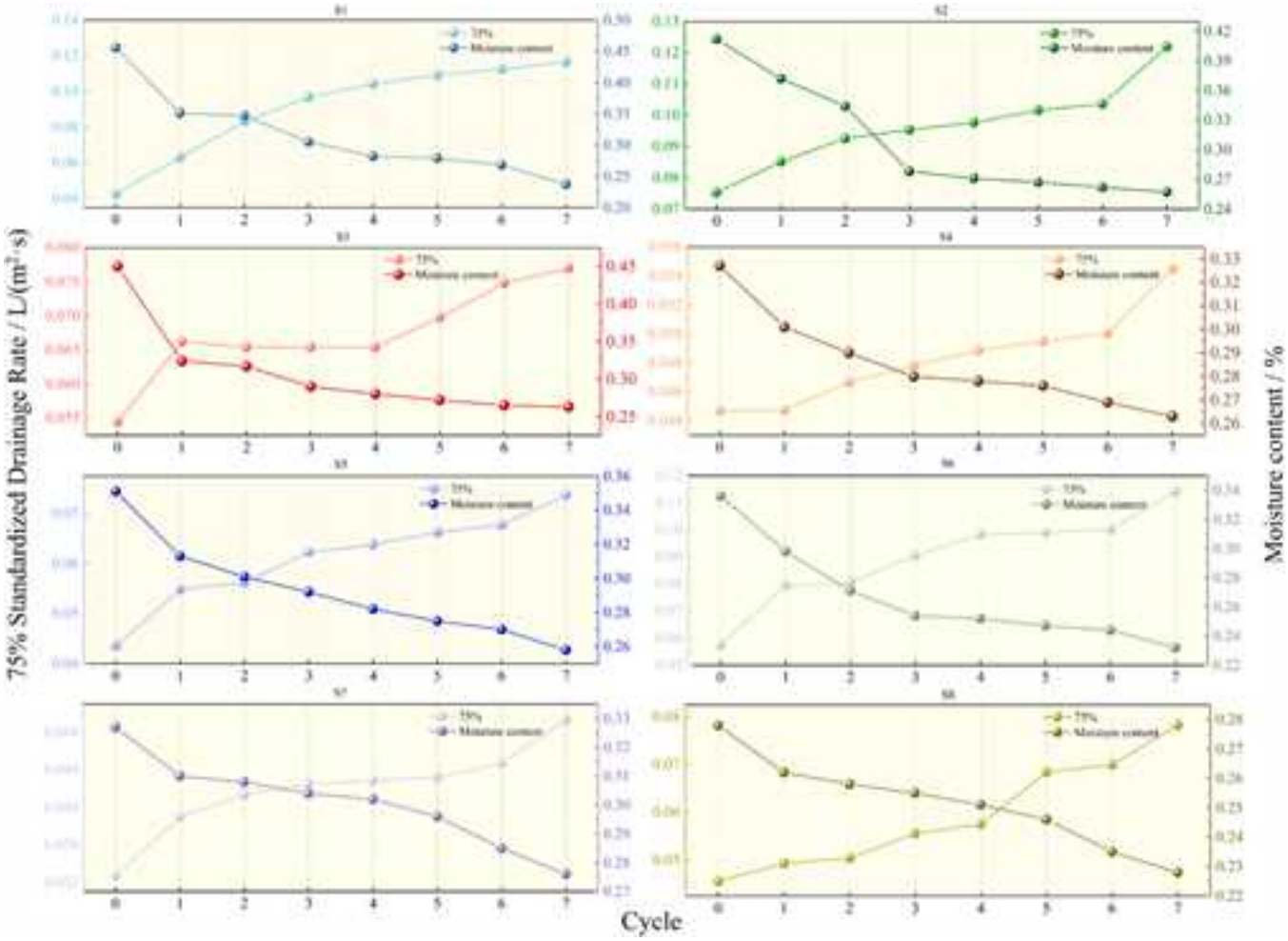

Fig. 7. Comparison of 75 % standard drainage rate and water content of eight foam samples under high and low temperature alternating aging.

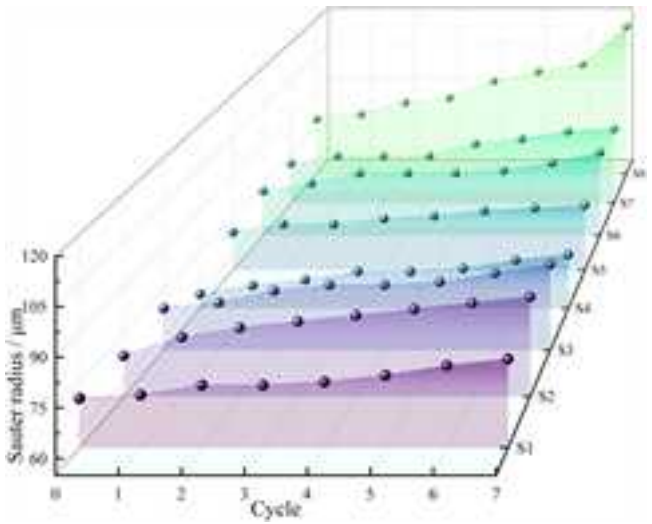

Fig. 8. Comparison of the initial Sauter radius of eight foam samples under high and low temperature alternating aging.

fuel. This results in a significant reduction in the foam's firefighting performance [27].

3.2. *Effect of high-low temperature alternating aging on foam foaming ability*

Foam expansion ratio is an indicator of foam foaming ability. However, solely considering the expansion ratio may not provide a comprehensive evaluation of foaming performance. A more complete characterization can be achieved by combining the expansion ratio with foam stability.

As shown in Fig. 9, S1 exhibits an overall decreasing trend. It has the highest initial expansion ratio of 10.7, but also the largest decline, with an overall reduction of approximately 14 %. This may be due to its high expansion ratio, where the gravitational synergy causes foam solution to accumulate at the bottom, leading to an uneven liquid content distribution and poor stability [6]. As a result, S1 shows a significant decline in the early stages, followed by a gradual and steady decrease in the later stages. S5 exhibits a gradual and stable decreasing trend. Although it has the lowest initial expansion ratio of 9.4, its decline is also the smallest, at approximately 4 %. This may be attributed to its lower expansion ratio, which reduces the impact of gravitational synergy, resulting in a more uniform liquid content distribution and better stability. Consequently,

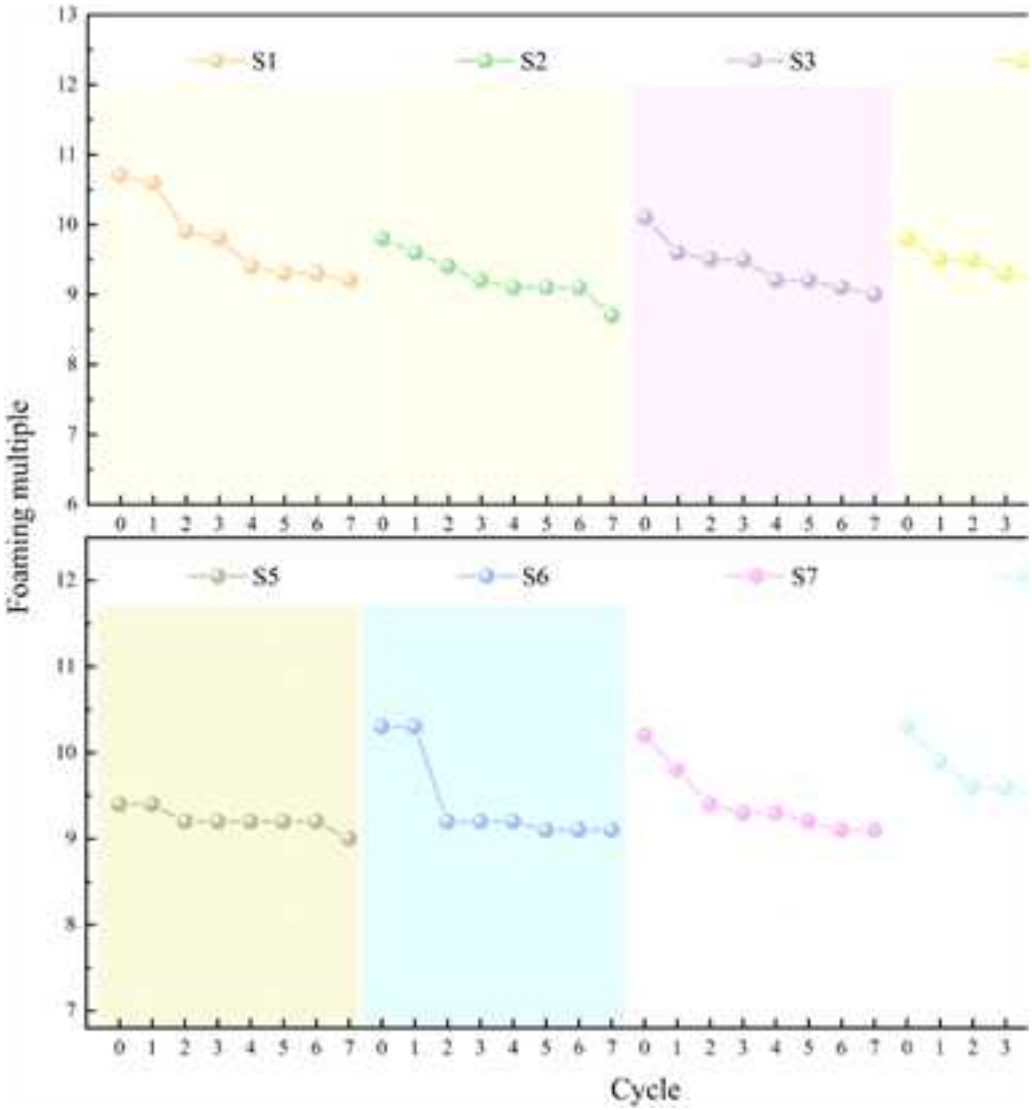

Fig. 9. Comparison of foam expansion ratio of eight foam samples under cyclic high-low temperature aging.

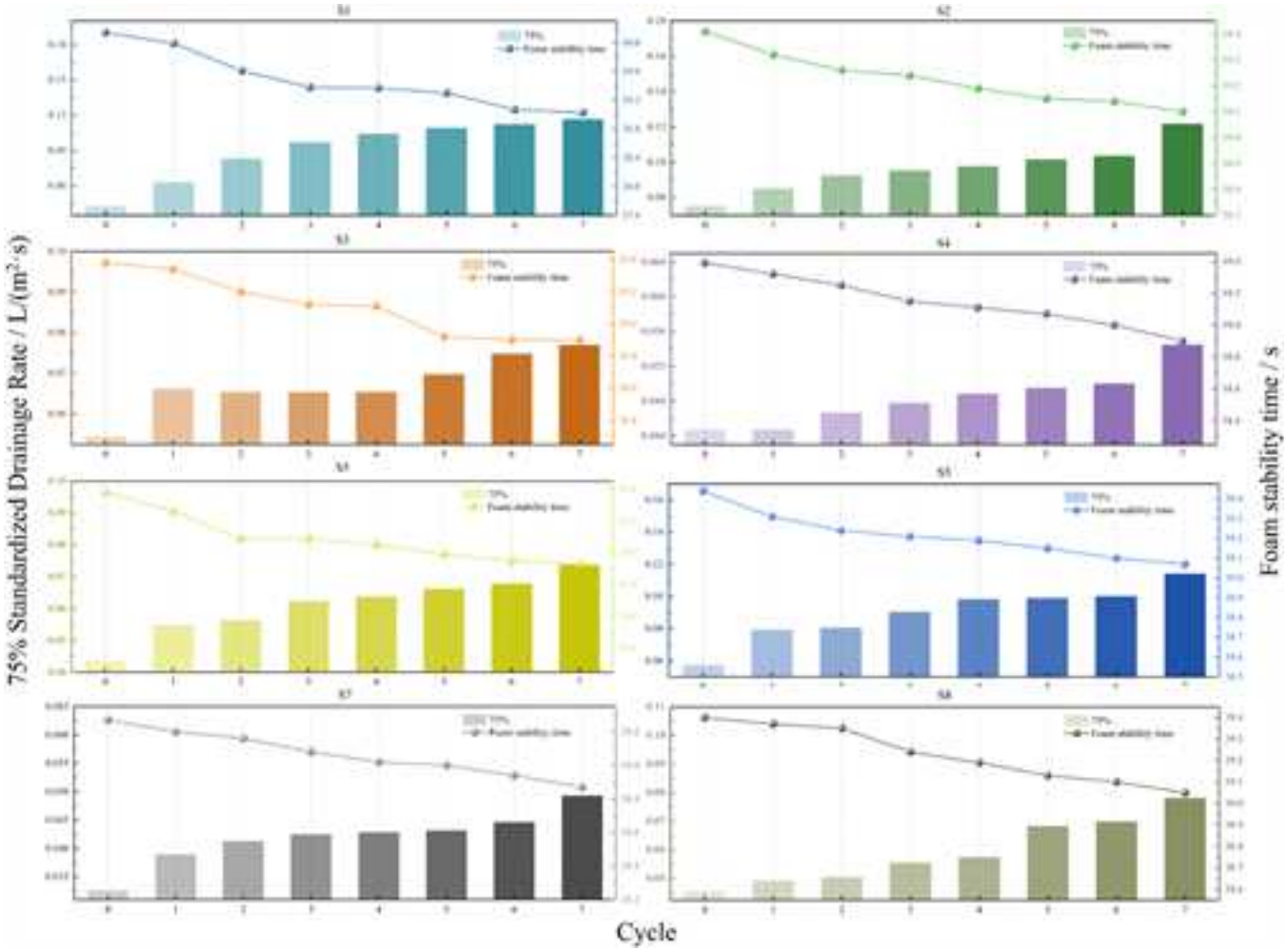

Fig. 10. Comparison of stability times of eight foam samples under cyclic high-low temperature aging.

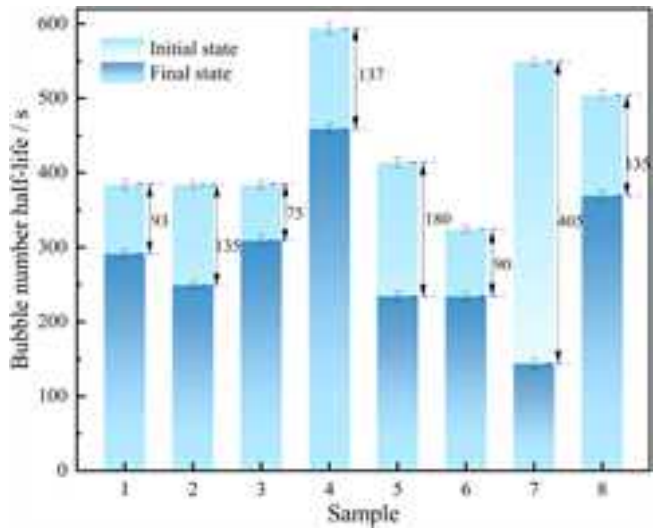

Fig. 11. Comparison of bubble count half-life of eight foam samples under cyclic high-low temperature aging.

S5 maintains a gradual and steady decline throughout the aging process. S6 initially shows a decreasing trend, with a sharp drop between cycles 1 and 2, followed by a stable trend after the second aging cycle. The overall expansion ratio decline for S6 is approximately 13 %. Other foams, which have an initial expansion ratio above 10, are significantly affected by gravitational synergy, leading to an uneven liquid content distribution. As a result, they exhibit a large initial decline, followed by a gradual and steady decrease in the later stages. The overall reduction in expansion ratio for these foam ranges from approximately 7–13 %.

As shown in Fig. 10, as the aging cycle increases, the foam stability time decreases with the increase in drainage rate. Among them, S1 has the best foam stability in the initial stage before aging, but the decline is also the most significant, with an overall decline of about 2.8 %. The remaining foams all show a gradual downward trend. The stability time of the foam is related to the foam stabilizer. It combines with the surfactant to form a weakly interacting polymer-surfactant system, and can also form a strongly interacting system. These systems enhance the stability of the foam by generating a strong spatial repulsive force [22–24]. The previous analysis shows that the uniformity of the solution is destroyed and the degradation of the stabilizer leads to a decrease in the content of the composite system. Therefore, the overall stability time decreases by about 0.79~1.24 %.

Both the foam expansion ratio and the stability time show a downward trend, indicating a clear correlation between them. This correlation may be due to the degradation of foam additive performance and gas-liquid interface properties caused by aging, which leads to a decrease in the overall foaming ability of the system [28–30]. On the one hand, the decline in foam expansion ratio leads to a decrease in the number of bubbles generated during the foaming process, limiting the volume and structural integrity of the foam. On the other hand, the

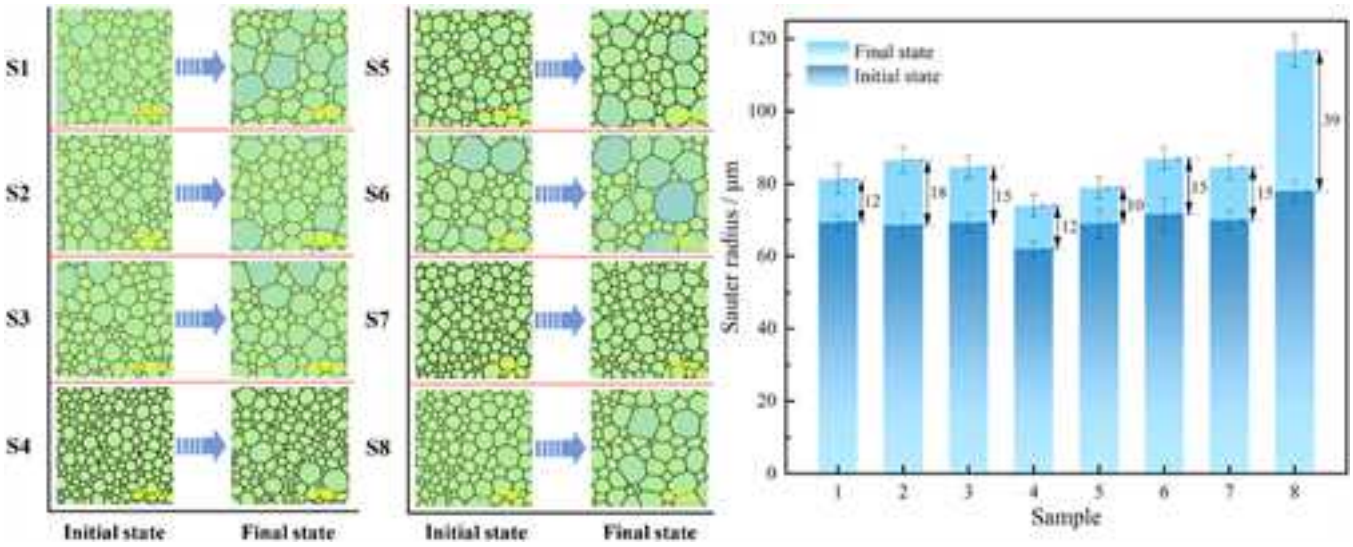

Fig. 12. Microscopic images captured by the foam scanner at different stages.

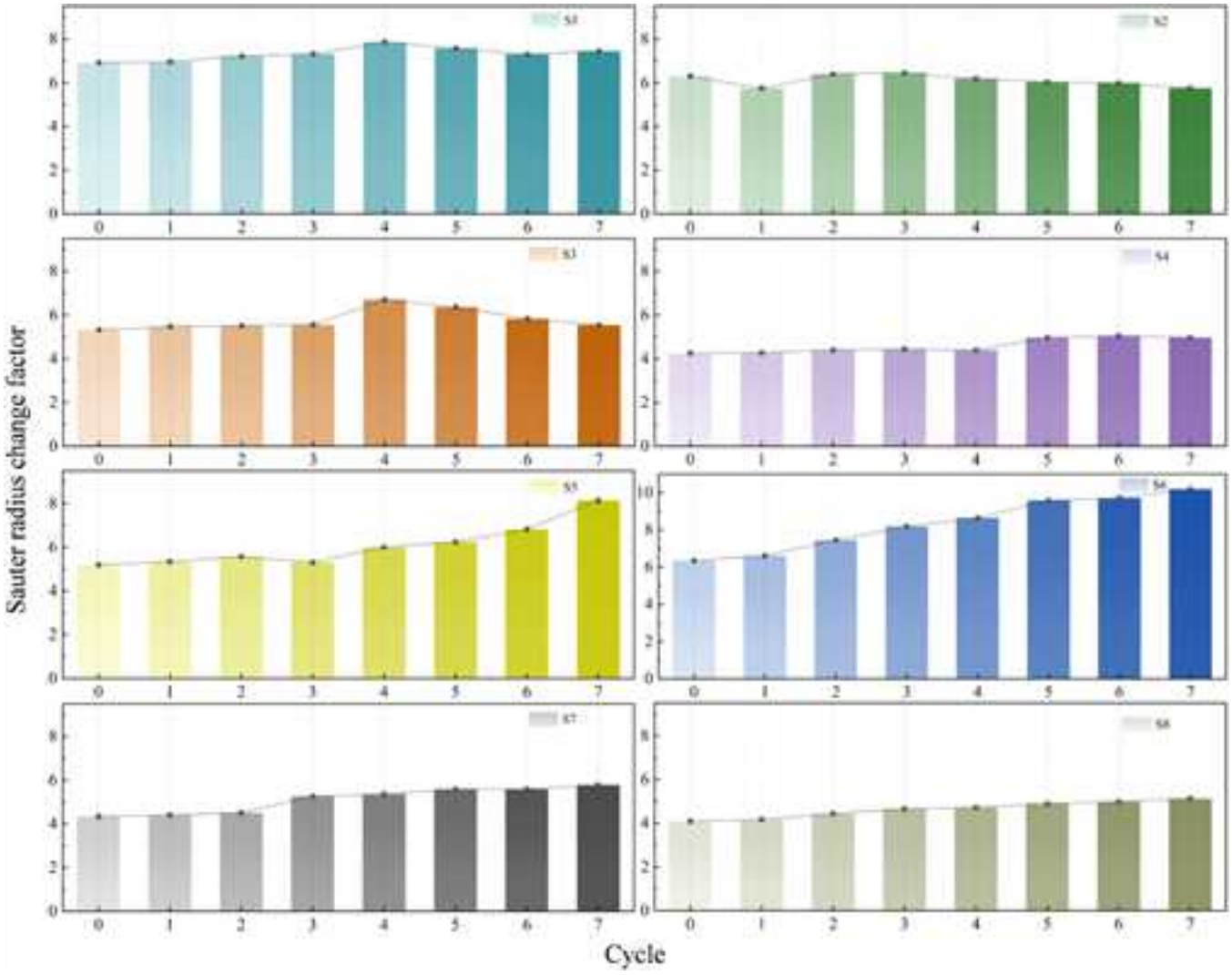

Fig. 13. Comparison of the change ratios of the Sauter radius of eight foam samples under cyclic high-low temperature aging.

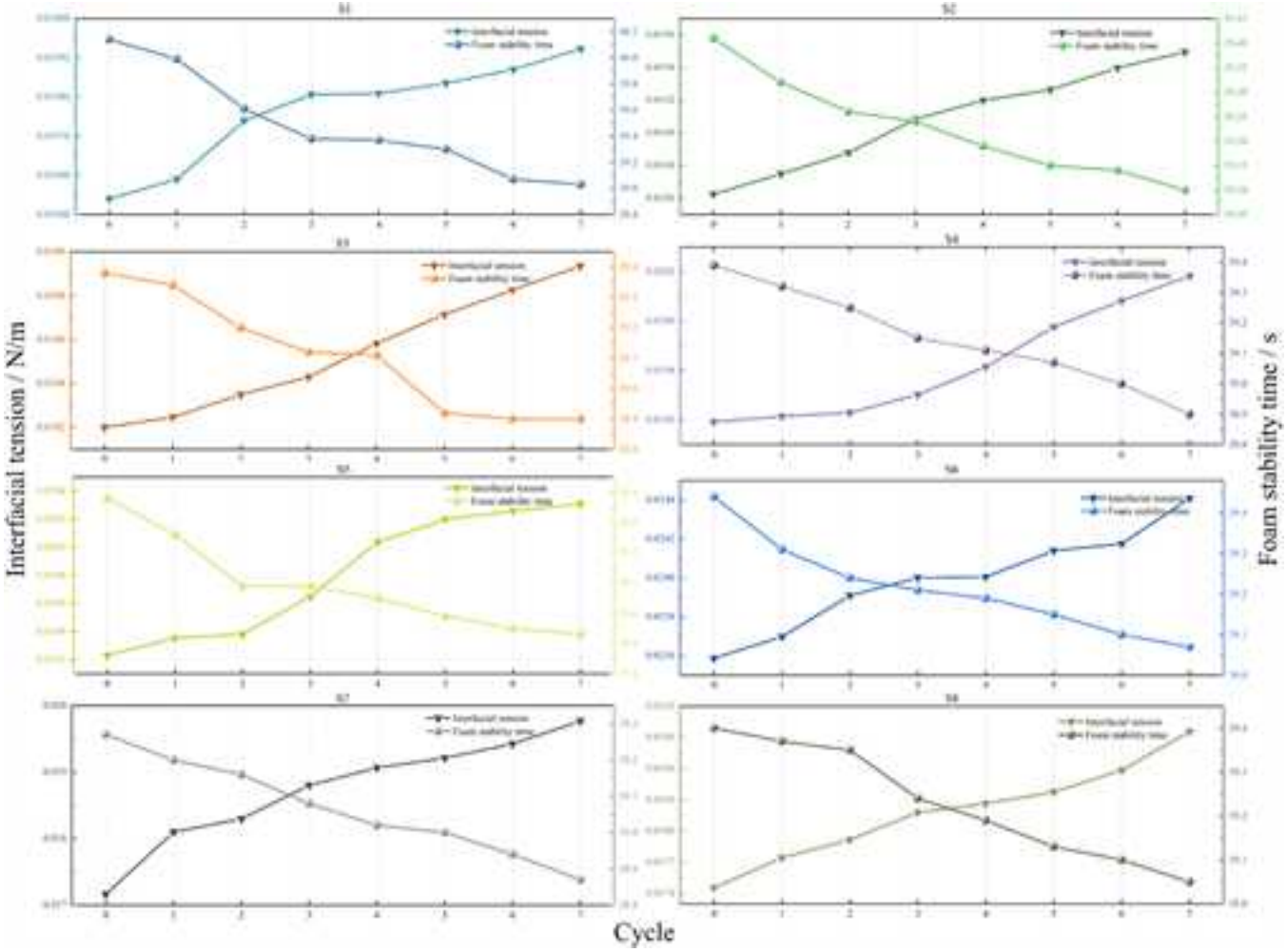

Fig. 14. Comparison of interfacial tension of eight foam samples under cyclic high-low temperature aging.

increase in drainage rate accelerates the drainage of liquid from the foam, further weakening the stability of the foam. The combined effect of the reduction in the number of bubbles and the accelerated drainage significantly weakens the overall foaming ability. Even if the initial expansion ratio is high, the rapid collapse of the foam will lead to a decrease in the effective expansion ratio. These changes reflect a significant decline in the foaming capacity of the foam system. The foam extinguishing agent fails to cover a sufficient fuel surface area within a given time. As a result, the extinguishing effect is impaired, and the suppression efficiency is reduced [31].

3.3. Effect of high-low temperature alternating aging on the stability of foam microstructure

In the study of foam performance, the stability of the microstructure is a key factor in evaluating the long-term usability and durability of the foam. The bubble count half-life and the variation rate of the bubble Sauter mean radius serve as important characterization indicators. These parameters comprehensively reflect the structural changes and stability of the foam over time.

The change rate of the average Sauter radius of foam can be calculated by the following formula:

$$\lambda = r_{32final} - r_{32initial} / r_{32initial} \times 100\% \quad (4)$$

Where: λ is the average Sauter radius change rate, %; $r_{32\ final}$ is final Sauter mean radius, μm.

As shown in Fig. 11, the bubble count half-life of different foam samples exhibits an overall downward trend during the aging cycle. Among them, S4 has the highest bubble count half-life before aging, demonstrating the best foam stability. Moreover, its overall decline during aging is relatively small, decreasing by approximately 22 % compared to the pre-aging state, indicating the most stable microstructure. S7 shows a relatively gradual decline in the early aging stages but experiences an abrupt drop of approximately 74 % in the fourth aging cycle. It shows poor resistance to aging and undergoes significant structural collapse. S6 has the lowest bubble count half-life before aging, but it exhibits the most gradual decline throughout the aging process, with an overall reduction of approximately 27.8 %. The other foam samples also show an overall downward trend, with reductions ranging from approximately 20–45 %. This may be due to the thermal stress on the foam structure during the aging process. This results in insufficient surface tension to maintain the overall foam structure, causing the foam system to become unstable and dramatically shortening the bubble half-life [26].

As shown in Fig. 12, the changes in the microstructure of eight types of AFFF before and after aging are presented. It can be observed from the figure that before aging, the microstructure of the foam extinguishant consists of uniformly distributed fine particles with well-defined boundaries and a relatively regular structure. After aging, significant changes occur in the microstructure, with noticeable particle coalescence to some extent. The particle size increases, the interfaces become progressively blurred, and some regions exhibit uneven particle distribution.

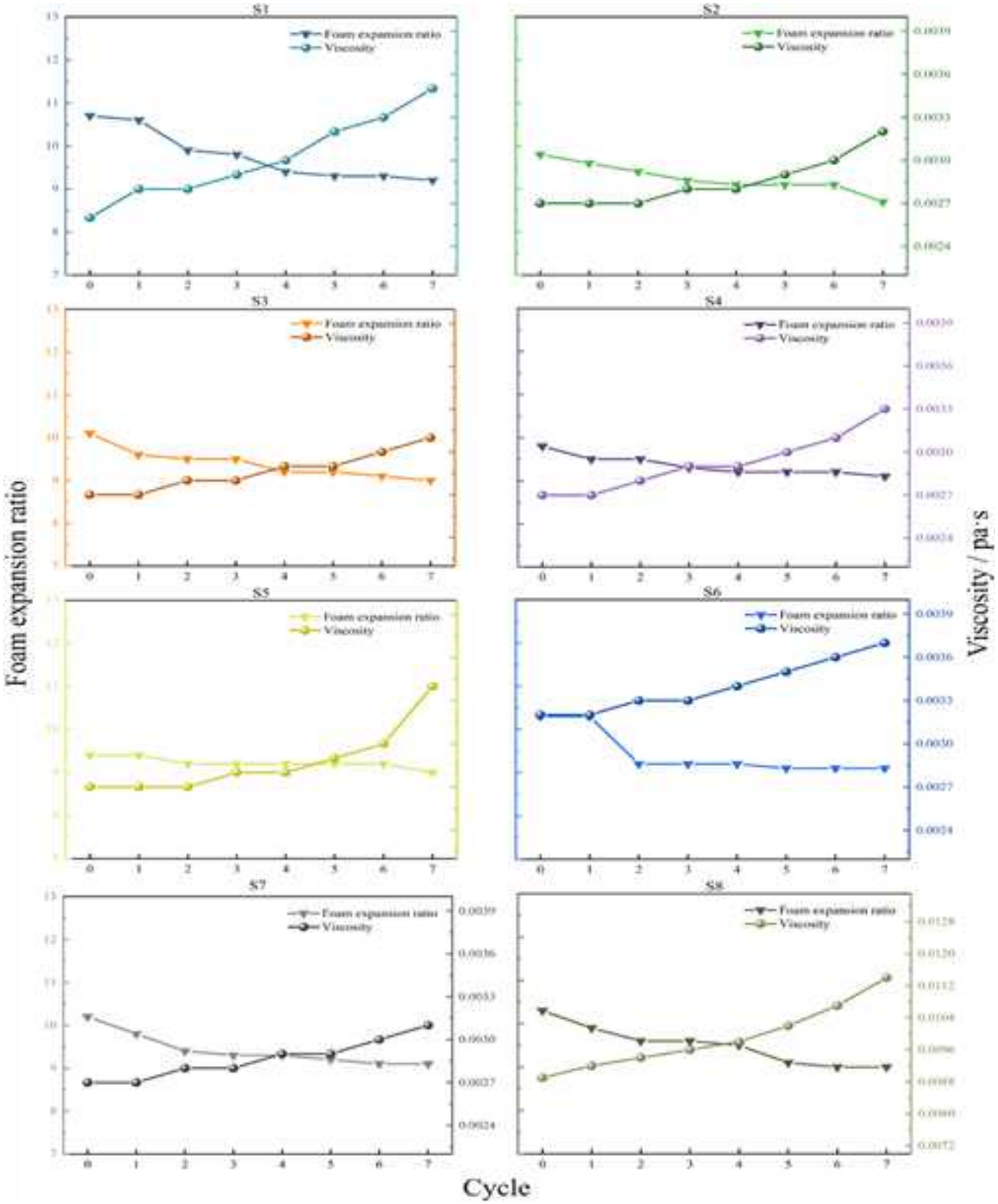

Fig. 15. Comparison of interfacial tension of eight foam samples under cyclic high-low temperature aging.

As shown in Fig. 13, the variation rate of the average radius of the foam Soter is generally increasing. The variation rate of the average radius of the foam Soter is defined as the ratio of the radius at the end of 75 % drainage to the radius at the end of foaming. Among them, the increase in the variation rates of S1, S2 and S6 is particularly obvious. This may be due to the significant decrease in the half-life of the bubble number, the accelerated bubble bursting rate, and the reduced overall stability of the foam. The weakening of the foam stability directly leads

Table 1
AFFF parameter units and dimension formula.

Parameter	Unit	Dimensionless Expression
T_f	s	T
T_{f0}	s	T
m	kg	M
ρ	kg/m^3	ML^{-3}
F	N/m	MT^{-2}
μ	Pa·s	ML^{-1}T^{-1}
n	/	/

to an increase in the bubble aggregation rate, an increase in the variation rate of the average radius of Soter, and a gradual coarsening of the foam structure. At the same time, the accelerated drainage rate leads to a further decrease in the liquid film strength, which accelerates the bubble bursting. Combined with the above reasons, the overall microstructural stability of the foam is significantly reduced during the aging cycle.

3.4. Effects of changes in foam physical and chemical properties on performance degradation

As shown in Fig. 14, with the extension of the aging cycles, the interfacial tension of the foams in all samples exhibits a gradual increase, while the foam stability time correspondingly decreases. This indicates that under high–low temperature alternation, the physicochemical properties of the foam solution deteriorate, leading to an increase in interfacial tension. A higher interfacial tension implies that the foam system requires more free energy to maintain the gas–liquid interface. Consequently, the stability of the liquid film is weakened, accelerating liquid drainage and thinning of the lamella, which ultimately makes the foam structure more prone to rupture [32]. It can thus be inferred that the increase in interfacial tension is strongly negatively correlated with the decline in foam stability. In other words, the higher the interfacial tension, the lower the foam stability, as reflected by a marked reduction in stability time.

As shown in Fig. 15, the viscosity exhibits an overall increasing trend with the extension of the aging cycles. Meanwhile, the foam expansion ratio decreases correspondingly. The increase in viscosity raises the energy consumption required for bubble formation, thereby hindering gas–liquid mixing and bubble refinement, which ultimately reduces the foam expansion ratio [33]. These results indicate that higher viscosity weakens the foaming ability of the system, manifested as a decline in the expansion ratio.

3.5. Dimensionless predictive model for the stability time of various AFFF after aging

Foam stability time is recognized as one of the critical indicators for evaluating the fire suppression effectiveness of foam extinguishing agents. During fire suppression, a foam layer is required to form a continuous coverage on the fuel surface to isolate oxygen, cool the combustibles, and prevent flame propagation. The stability of the foam directly determines its firefighting performance [34]. However, varying stability durations are observed among different AFFF products due to differences in chemical composition, formulation design, and component concentrations. To accurately predict the stability time of aged AFFF solutions, a predictive model will be developed through dimensionless analysis combined with experimental datasets.

The aged stability time T_f is correlated with six variables: the initial foam stability timeT_{f0}; the ratio of aging time to shelf-life t; foam mass m; foam density ρ; surface tension F; and gas-to-liquid ratio R. This relationship is mathematically represented by Eq. (5).

$$f\left(T_{f0}, T_f, t, \rho, F, n\right) = 0 \tag{5}$$

The basic factors used include: length (L), mass (M), time (T). Basic physical quantities: T_{f0}, ρ, μ.

List the dimensionless equations:

$$\begin{cases} \pi_1 = T_{f0}^{\alpha_1} m^{\beta_1} \rho^{\gamma_1} T_f = [T]^{\alpha_1} [M]^{\beta_1} \left[ML^{-3}\right]^{\gamma_1} T \\ \pi_2 = T_{f0}^{\alpha_2} m^{\beta_2} \rho^{\gamma_2} F = [T]^{\alpha_2} [M]^{\beta_2} \left[ML^{-3}\right]^{\gamma_2} MT^{-2} \\ \pi_3 = T_{f0}^{\alpha_3} m^{\beta_3} \rho^{\gamma_3} m = [T]^{\alpha_3} [M]^{\beta_3} \left[ML^{-3}\right]^{\gamma_3} M \\ \pi_4 = T_{f0}^{\alpha_4} m^{\beta_4} \rho^{\gamma_4} n = [T]^{\alpha_4} [M]^{\beta_4} \left[ML^{-3}\right]^{\gamma_4} n \end{cases} \tag{6}$$

Get dimensionless:

$$\begin{cases} \pi_1 = T_f / T_{f0} \\ \pi_2 = m\sqrt{\rho} \Big/ \sqrt[2]{T_{f0}^3} \sqrt[2]{\mu^3} \\ \pi_3 = F\sqrt{T_{f0}}\sqrt{\rho} \Big/ \sqrt[2]{\mu^3} \\ \pi_4 = n \end{cases} \tag{7}$$

Further simplifying:

$$T_f / T_{f0} = f(FT_{f0}^2 \Big/ mn \times 10^{-2}) \tag{8}$$

In order to accurately predict the stability time of foam under different aging cycles, this study uses a nonlinear fitting method to optimize the experimental data. Based on the given data, the power function is used as an example:

$$y = ax^b \tag{9}$$

Let $\lambda = FT_{f0}^2 / mn \times 10^{-2}$, and use it as the independent variable in the dimensionless prediction model, then we have formula (10):

$$T_f / T_{f0} = a\lambda^b \tag{10}$$

Where: a and b are constants.

Based on the experimentally measured foam stability time data for the eight foam samples, a fitting analysis was conducted on the dimensionless parameters. Consequently, a dimensionless predictive model for the ratio of foam stability time to initial foam stability time was established, as shown in Fig. 16.

4. Conclusion

Due to the aqueous film-forming foam extinguishing agent needs to be stored for a long period of time, it is inevitable that it will face the problem of aging and failure during the storage process. Therefore, this paper investigates the effect of aging cycle on foam drainage performance, foaming ability and microstructure stability by alternating high and low temperature aging test. According to the analysis of the test results, the following conclusions are drawn:

(1) Alternating high and low-temperature aging significantly affects the drainage performance of the foam. The increase in the standardized foam drainage rate ranges from 0.22 t to 1.73 times. The water content decreases by 18–92.4 %. The initial Sauter mean radius increases by 14.5–50 %. The changes in these three parameters form a comprehensive feedback mechanism, which can serve as an important indicator for evaluating the aging resistance of AFFF.
(2) High and low temperature alternating aging significantly affects the foaming ability of foam and accelerates the collapse of foam. With the increase of aging cycle, the overall decrease range of foaming multiple is about 4–14 %. The decrease range of foam stability time is about 0.79–2.8 %. The changes in the two reflect the synergistic degradation effect of high and low temperature alternating aging on foaming performance and foam durability.

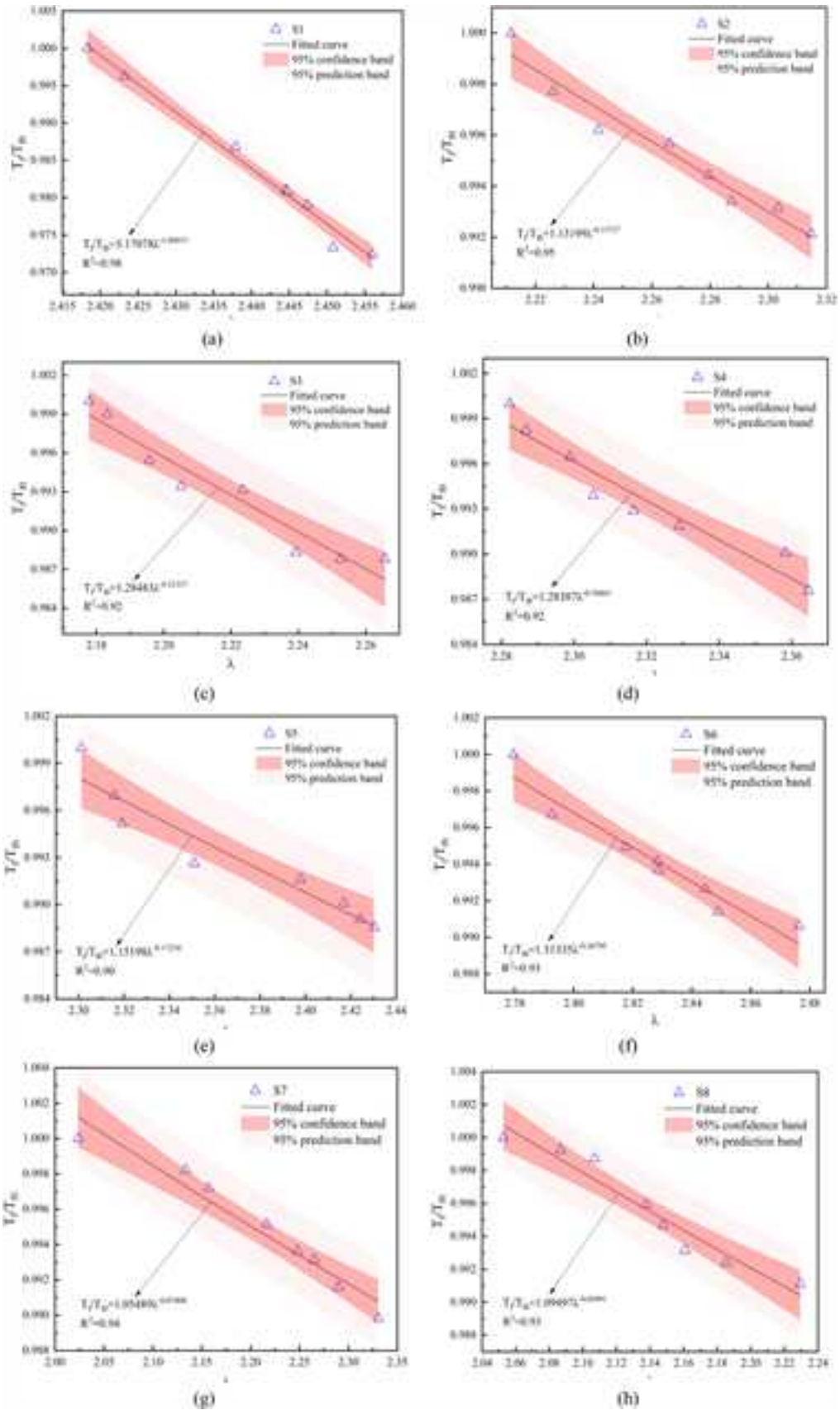

Fig. 16. Dimensionless prediction model for the stability time of aged foams. (a) S1 (b) S2 (c) S3 (d) S4 (e) S5 (f) S6 (g) S7 (h) S8.

(3) With the increase of aging cycle, the half-life of bubble number decreases by about 20–74 %. Combining the analysis of 75 % standardized drainage rate, bubble number half-life and Sauter radius change ratio, a dynamic feedback mechanism is formed, which can be used as an important indicator for evaluating the stability of foam microstructure.
(4) A dimensionless predictive model for the stability time of AFFF under alternating high and low-temperature aging was developed using the dimensional analysis method.

CRediT authorship contribution statement

Zhengyang Wang: Formal analysis, Data curation. **Peiyao Chen:** Investigation, Conceptualization. **Hideki Yoshioka:** Methodology, Formal analysis. **Kai Wang:** Supervision, Project administration, Funding acquisition. **Qihang Yue:** Writing – review & editing, Data curation. **Junyi Zhang:** Writing – original draft, Methodology, Investigation, Data curation. **Biao Zhou:** Writing – review & editing, Validation, Conceptualization. **Shanlong Wang:** Supervision, Conceptualization. **Yafei Zhou:** Software, Conceptualization. **Wei Wang:** Writing – review & editing, Conceptualization.

Declaration of Competing Interest

The authors declared that they have no conflicts of interest to this work.

Acknowledgment

This work is supported by Beijing Municipal Science and Technology Project (Z231100003823022), Tianjin Natural Science Foundation Project (22JCZDJC00880; 22JCZDJC00900), the Ordos key research and development program (No.YF20240026), Key-Area Research and Development Program of Guangdong Province (2024B1111080002), Tianjin Applied Basic Research Multiple Investment Foundation-Urban Fire Protection Project (22JCYBJC01730), the Fundamental Research Funds for the Central Universities (No. 2025ZKPYAQ03) and Beijing Nova Program (No. 202504841008).

Data availability

Data will be made available on request.

References

[1] Z. Wang, X. Jiang, C. Yang, D. Wang, B. Zhou, W.J.F. Wang, Experimental study on the quantitative evaluation of the thermal stability performance and heat insulation characteristics of fire-fighting foam, Materials 48 (2024) 353–366.
[2] Y. Li, G. Luan, Q. Jing, X. Li, C. Yan, Y. Li, T.S. Zhang, Experimental study of the effect of crude oil water content on boilover fire, Int. J. Therm. Sci. 206 (2024) 109328.
[3] B.Z. Dlugogorski, T.H. Schaefer, Compatibility of aqueous film-forming foams (AFFF) with sea water, Fire Saf. J. 120 (2021) 103288.
[4] C.A. Moody, J.A. Field, Perfluorinated surfactants and the environmental implications of their use in fire-fighting foams, Environ. Sci. Technol. 34 (2000) 3864–3870.
[5] X. Jia, Reseach progess of aqueous film-forming foam extinguishing agent 24 (2015).
[6] S. Magrabi, B. Dlugogorski, G.J. Jameson, The performance of aged aqueous foams for mitigation of thermal radiation, Dev. Chem. Eng. Miner. Process. 8 (2000) 93–112.
[7] D. Kong, D. Wang, J. Chen, J. Zhang, X. He, B. Li, X. He, H. Liu, Assessing the mixed foam stability of different foam extinguishing agents under room temperature and thermal radiation: an experimental study, J. Mol. Liq. 369 (2023) 120805.
[8] K. Hinnant, S. Giles, E. Smith, A. Snow, R.J. Ananth, Characterizing the role of fluorocarbon and hydrocarbon surfactants in firefighting-foam formulations for fire-suppression, Fire Technol. 56 (2020) 1413–1441.
[9] X. Yu, X. Yu, Y. Lin, H. Li, G. Li, R.J.L. Zong, Comparative study on interfacial properties, foam stability, and firefighting performance of c6 fluorocarbon surfactants with different hydrophilic groups, Langmuir ACS J. Surf. Colloids 39 (2023) 16336–16348.
[10] Z. Wang, X. Jiang, C. Yang, B.J. Zhou, Experimental study on thermal stability and burn-back performance of aqueous film forming foam agent (AFFF) with short-chain fluorocarbon surfactant or flame retardant, Fire Saf. J. 146 (2024) 104135.
[11] W. Kang, L. Yan, F. Ding, Z.J.C. Xu, Effect of polysaccharide polymers on the surface and foam properties of aqueous film-forming foam, Colloid Interface Sci. Commun. 45 (2021) 100540.
[12] Y. Sheng, N. Jiang, X. Sun, S. Lu, C. Li, Experimental study on effect of foam stabilizers on aqueous film-forming foam, Fire Technol. 54 (2018) 211–228.
[13] N.F. Khanyi, The impact of the storage facility on performance parameters of Aqueous Film-Forming Fire-Fighting Foam (AFFF) in aviation fire protection, 2023.
[14] S. Magrabi, B.Z. Dlugogorski, G.J. Jameson, A comparative study of drainage characteristics in AFFF and FFFP compressed-air fire-fighting foams, Fire Saf. J. 37 (2002) 21–52.
[15] Y. Sheng, S. Lu, N. Jiang, X. Wu, C. Li, Drainage of aqueous film-forming foam stabilized by different foam stabilizers, J. Dispers. Sci. Technol. 39 (2018) 1266–1273.
[16] B.Z. Dlugogorski, S. Phiyanalinmat, E.M.J. Kennedy, Dynamic surface and interfacial tension of AFFF and fluorine-free class b foam solutions, Fire Saf. Sci. 8 (2005) 719–730.
[17] H. Li, X. Yu, K. Qiu, B. Bo, Q. Li, S.J. Lu, Role of salts in fire extinguishing performance of aqueous film-forming foam (AFFF), Case Stud. Therm. Eng. 49 (2023) 103159.
[18] P. Amani, S.I. Karakashev, N.A. Grozev, S.S. Simeonova, R. Miller, V. Rudolph, M. Firouzi, Effect of selected monovalent salts on surfactant stabilized foams, Adv. Colloid Interface Sci. 295 (2021) 102490.
[19] G. Racz, E. Erdös, K.J.C. Koczo, P. Science, Measurement of pressure distribution in the plateau borders of fresh and aged foams, Colloid Polym. Sci. 260 (1982) 720–725.
[20] J. Gniazdowska, A. Rabajczyk, P. Stojek, T. Wilczyński, Expired foam extinguishing agents and evaluation of their suitability for further use, Zesz. Nauk. SGSP 1 (2024) 61–74.
[21] J.L. Scheffey, R.L. Darwin, J.T. Leonard, Evaluating firefighting foams for aviation fire protection, Fire Technol. 31 (1995) 224–243.
[22] B.M. Folmer, B. Kronberg, Effect of surfactant- polymer association on the stabilities of foams and thin films: sodium dodecyl sulfate and poly (vinyl pyrrolidone, Langmuir 16 (2000) 5987–5992.
[23] R. Petkova, S. Tcholakova, N.J.C. Denkov, Role of polymer–surfactant interactions in foams: effects of ph and surfactant head group for cationic polyvinylamine and anionic surfactants, Colloids Surf. A Physicochem. Eng. Asp. 438 (2013) 174–185.
[24] R. Petkova, S. Tcholakova, N. Denkov, Foaming and foam stability for mixed polymer–surfactant solutions: effects of surfactant type and polymer charge, Langmuir ACS J. Surf. Colloids 28 (2012) 4996–5009.
[25] T. Liddicoet, L. Smithson, Analysis of surfactants using pyrolysis-gas chromatography, J. Am. Oil Chem. Soc. 42 (1965) 1097–1102.
[26] L. Sun, W. Pu, J. Xin, P. Wei, B. Wang, Y. Li, C. Yuan, High temperature and oil tolerance of surfactant foam/polymer–surfactant foam, RSC Adv. 5 (2015) 23410–23418.
[27] S. Magrabi, B.Z. Dlugogorski, G. Jameson, A comparative study of drainage characteristics in AFFF and FFFP compressed-air fire-fighting foams, Fire Saf. J. 37 (2002) 21–52.
[28] D. Beneventi, B. Carre, A. Gandini, Role of surfactant structure on surface and foaming properties, Colloids Surf. A Physicochem. Eng. Asp. 189 (2001) 65–73.
[29] G.C. Sawicki, Impact of surfactant composition and surfactant structure on foam control performance, Colloids Surf. A Physicochem. Eng. Asp. 263 (2005) 226–232.
[30] H. Wang, W. Guo, C. Zheng, D. Wang, H. Zhan, Effect of temperature on foaming ability and foam stability of typical surfactants used for foaming agent, J. Surfactants Deterg. 20 (2017) 615–622.
[31] M. Lou, H. Jia, Z. Lin, D. Zeng, J. Huo, Study on fire extinguishing performance of different foam extinguishing agents in diesel pool fire, Results Eng. 17 (2023) 100874.
[32] Z. Wang, S. Li, D. Peng, H. Cheng, Y. Wei, The effect of interfacial tension on CO2 oil-based foam stability under different temperatures and pressures, Fuel 341 (2023) 127755.
[33] T. Ivana, B. Karol, P.J.S. Marzena, The effect of firefighting foams on the environment and fire extinguishing, Fire Technol. 25 (2012) 29–36.
[34] Y. Sheng, Y. Peng, H. Zhang, C. Yan, Y. Li, Effect of SiO2 nanoparticles on foam stability of Environmental-friendly firefighting foam, Chem. Eng. Sci. 37 (2023) 22050272–22050276.